

# Accurate determination of atomic structure of multiwalled carbon nanotubes by nondestructive nanobeam electron diffraction

Zejian Liu

Department of Physics and Astronomy, University of North Carolina at Chapel Hill, Chapel Hill, North Carolina 27599-3255

Qi Zhang

Department of Physics and Astronomy, University of North Carolina at Chapel Hill, Chapel Hill, North Carolina 27599-3255

Lu-Chang Qin<sup>a)</sup>

Department of Physics and Astronomy, University of North Carolina at Chapel Hill, Chapel Hill, North Carolina 27599-3255 and Curriculum in Applied and Materials Sciences, University of North Carolina at Chapel Hill, Chapel Hill, North Carolina 27599-3255

(Received 29 October 2004; accepted 16 March 2005; published online 2 May 2005)

We report a method that allows direct, systematic, and accurate determination of the atomic structure of multiwalled carbon nanotubes by analyzing the scattering intensities on the nonequatorial layer lines in the electron diffraction pattern. Complete structure determination of a quadruple-walled carbon nanotube is described as an example, and it was found that the intertubular distance varied from 0.36 nm to 0.5 nm with a mean value of 0.42 nm.

© 2005 American Institute of Physics. [DOI: 10.1063/1.1923170]

Carbon nanotubes possess many extraordinary physical and chemical properties and have attracted intense attention since their discovery.<sup>1-3</sup> A single-walled carbon nanotube can be characterized by its diameter and helicity or, equivalently, by the integer chiral indices  $[u, v]$ , which define the perimeter vector  $\mathbf{A}$  on graphene by  $\mathbf{A} = [u, v] = u\mathbf{a}_1 + v\mathbf{a}_2$  ( $\mathbf{a}_1$  and  $\mathbf{a}_2$  are the crystallographic basis vectors with magnitude  $a_1 = a_2 = a_0 = 0.2461$  nm and interangle  $60^\circ$ ).<sup>4</sup> A single-walled carbon nanotube is metallic if  $u - v$  is divisible by 3; otherwise, it is semiconducting unless the diameter is extremely small where all nanotubes appear metallic.<sup>5-7</sup> A multiwalled carbon nanotube consists of multiple concentric single-walled nanotubes. It is necessary to measure both the diameter and helicity or, equivalently, the chiral indices  $[u, v]$  of each and every shell within the nanotube in order to determine the atomic structure of a multiwalled carbon nanotube. Although great progress has been made in determining the atomic structure of single-walled carbon nanotubes,<sup>8-12</sup> few direct measurements of the atomic structure of multiwalled carbon nanotubes have been available.<sup>13,14</sup>

Electron diffraction, especially nanobeam electron diffraction (NBD) has been a powerful technique in determining the atomic structure of carbon nanotubes. It offers a great advantage over other local probe techniques, such as scanning tunneling microscopy or atomic force microscopy, in that it allows not only the structure determination of the outermost shell, but also the interior shells of the nanotube. Moreover, NBD performed at a lower accelerating voltage (below the threshold voltage of 86 kV for knock-on damage to carbon nanotubes by the incident fast electrons) provides the capability of locating a specific nanotube and determining its atomic structure before we measure its properties.<sup>15-17</sup>

Here, we report the accurate determination of the atomic structure of multiwalled carbon nanotubes by a nondestructive

NBD technique. A quadruple-walled carbon nanotube has been unambiguously determined as an example. The method developed here is general and can be used to determine the atomic structure of multiwalled carbon nanotubes consisting of up to 15 concentric shells. To avoid knock-on damage to the carbon nanotubes, the electron microscope (JEM-2010F equipped with a field emission gun) was operated at 80 kV and a parallel electron illumination with a 20 nm beam that was formed by utilizing a 10  $\mu\text{m}$  condenser aperture and exciting the first condenser lens to maximum. The NBD patterns were recorded initially on photographic films, which were later digitized with a high-resolution film scanner for quantitative analysis.

In an electron diffraction pattern, only the principal layer lines that contain the  $\{100\}^*$ -type Bragg reflections have significant intensities, as schematically illustrated in Fig. 1. The layer line index,  $\ell$ , and the order of Bessel functions,  $n$ , are

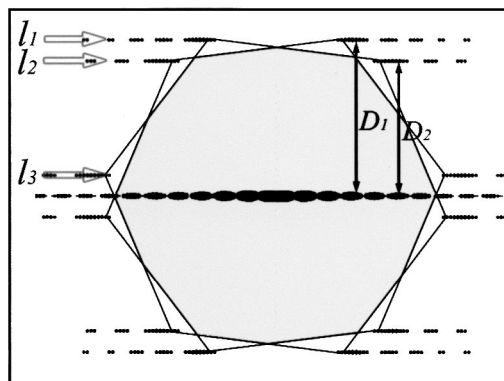


FIG. 1. Calculated electron diffraction pattern of a chiral single-walled carbon nanotube of the helicity  $\alpha$ . The two hexagons represent the principal reflections of graphene and form three principal layer lines above and below the equatorial line.  $D_1$  and  $D_2$  specify the layer line spacings. The relative twist angle is related, but not equal to the helical angle. The helicity can be calculated  $\alpha = \tan^{-1}[(2D_2 - D_1)/\sqrt{3}D_1]$  and the ratio of chiral indices is  $v/u = (2D_2 - D_1)/(2D_1 - D_2)$ .

<sup>a)</sup> Author to whom correspondence should be addressed; electronic mail: lcqin@physics.unc.edu

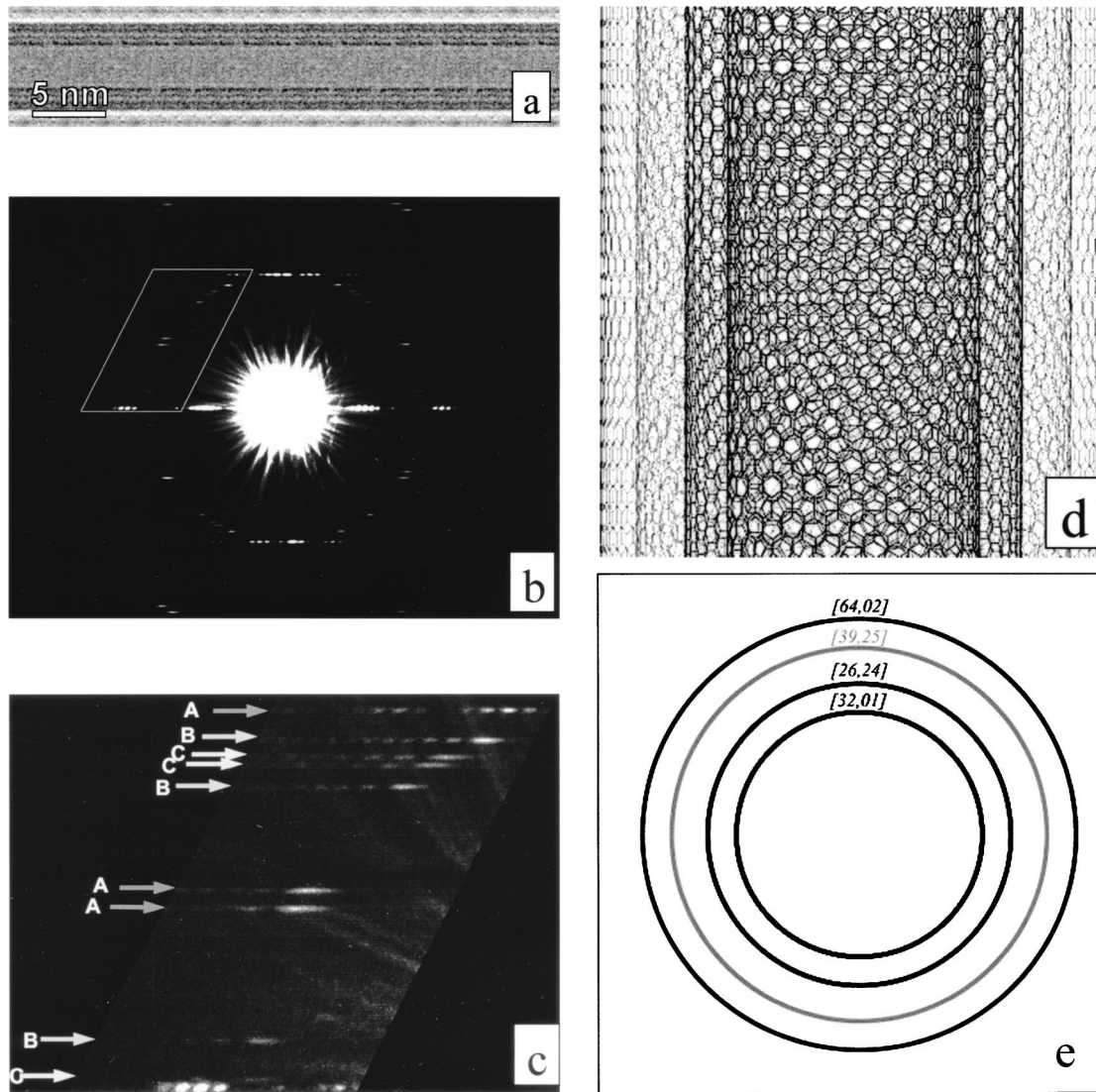


FIG. 2. (a) Transmission electron microscope image of a quadruple-walled carbon nanotube showing four walls on each side of the hollow core. The inner diameter and outer diameter of this nanotube is about 2.6 nm and 5.0 nm, respectively. (b) Electron diffraction pattern of the quadruple-walled carbon nanotube. (c) Magnified view of the enclosed region in (b). Three different helicities of  $1.53^\circ$ ,  $22.84^\circ$ , and  $28.76^\circ$ , are determined from the nine layer lines indicated by arrows labeled as A, B, and C, respectively. The modulated diffraction intensity distribution on the layer lines corresponding to helicity of  $1.53^\circ$  are due to the overlap of contributions from two shells of different diameters but the same helicity. (d) Side view of the atomic structure of the quadruple-walled carbon nanotube with the chiral indices  $[32,1]$ ,  $[26,24]$ ,  $[39,25]$ , and  $[64,2]$ . All shells are semiconducting. (e) Cross-sectional view of the structure of the quadruple-walled carbon nanotube with varying intertubular distances.

related by the selection rule for carbon nanotube  $[u, v]$

$$\ell = \frac{n(u+2v) + 2m(u^2 + v^2 + uv)}{uM}, \quad (1)$$

where  $m$  is an integer and  $M$  is the maximum common divisor of  $(2u+v)$  and  $(2v+u)$ . The selection rule also implies that  $n$  can only be multiples of the maximum common divisor of  $u$  and  $v$ . From the theory of electron diffraction from carbon nanotubes,<sup>18,19</sup> the scattering intensity distribution on a layer line is dominated only by a single Bessel function. By examining the geometry of the simulated electron diffraction pattern shown in Fig. 1, we can deduce that the electron intensity distributions on layer lines  $\ell_1$ ,  $\ell_2$ , and  $\ell_3$  indicated by the arrows can be expressed by the Bessel functions of orders related to the chiral indices  $[u, v]$ :<sup>20</sup>  $I_{\ell_1} \propto |J_v(\pi dR)|^2$ ,  $I_{\ell_2} \propto |J_u(\pi dR)|^2$ , and  $I_{\ell_3} \propto |J_{u+v}(\pi dR)|^2$ , respectively, where  $d$  is the nanotube diameter and  $R$  is the radial distance measured from the central vertical axis in the electron diffraction

pattern. The order of the responsible Bessel function can be identified from the intensity distribution, for example, the ratio of the peak positions that is unique to each order of Bessel function. To achieve high accuracy, complementary relations are also used, such as the following:

$$\frac{v}{u} = \frac{(2D_2 - D_1)}{(2D_1 - D_2)}, \quad (2)$$

where  $D_1$  is the spacing between the first principal layer line and the equatorial line, and  $D_2$  is the spacing between the second principal layer line and the equatorial line, as schematically shown in Fig. 1. When the layer lines are read from the digitized data, the uncertainties in measuring the ratio  $v/u$  can be reduced to less than 0.2%. Having determined  $v$  and  $v/u$ , we can assign the carbon nanotube its chiral indices  $[u, v]$ , and the true diameter  $d$  and helicity  $\alpha$  of this nanotube can then be calculated directly from the chiral indices by  $d = a_0 \sqrt{u^2 + v^2 + uv} / \pi$  and  $\alpha = \cos^{-1}[(2u+v) / 2\sqrt{u^2 + v^2 + uv}]$ .

For a multiwalled carbon nanotube, it is necessary to determine the chiral indices  $[u_j, v_j]$  for each individual shell  $j$ . Once all the chiral indices are determined, the intertubular distances between the neighboring shells in the nanotube can also be obtained.

Figure 2(a) shows the transmission electron microscopy (TEM) image of a quadruple-walled carbon nanotube with an inner diameter and outer diameter of 2.6 nm and 5.0 nm, respectively. Four dark image lines corresponding to the nanotube walls can be observed on each side of the tubule. Since the electron microscope was operated at 80 kV, at which the point resolution of the microscope is 0.34 nm, it would be difficult to obtain accurate measurement of the shell diameters from the TEM image. However, the electron diffraction pattern of this nanotube, shown in Fig. 2(b), can offer accurate measurement of both the diameter and helicity of each individual shell. Three different helicities can be obtained by examining the number of principal diffraction layer lines indicated by the arrows labeled as A, B, and C in the electron diffraction pattern. By measuring the principal layer line spacings in the electron diffraction pattern in Fig. 2(b), we can determine the three helicities:  $1.53^\circ$  (A arrows),  $22.84^\circ$  (B arrows), and  $28.76^\circ$  (C arrows), respectively. Since there are four individual shells in the nanotube, two shells must have the same helicity. These two shells are identified by the modulations in the intensity distribution on the layer line marked with A arrows (helicity  $1.53^\circ$ ), which indicate that two nanotubes have both contributed to these layer lines. The  $v/u$  ratios were also measured to be 0.031, 0.642, and 0.927 for the helicities  $1.53^\circ$ ,  $22.84^\circ$ , and  $28.76^\circ$ , respectively. Using the principal layer line  $\ell_1$  and the positions of the intensity peaks on this layer line, the value of index  $v$  can be deduced:  $v=25$  for the helicity of  $22.84^\circ$  and  $v=24$  for the helicity of  $28.76^\circ$ . Combined with the  $v/u$  ratios determined above, the chiral indices for these two nanotubes are assigned to be  $[26,24]$  and  $[39,25]$ , respectively, which are neighboring shells in the nanotube.

The other two nanotubes with the same helicity  $1.53^\circ$  are determined to have chiral indices  $[32,1]$  and  $[64,2]$ , making use of the geometric constraints of the concentric shells in the multiwalled carbon nanotube. Figure 2(d) shows the determined structure in side view of the four shells of this nanotube with chiral indices  $[32,1]$ ,  $[26,24]$ ,  $[39,25]$ , and  $[64,2]$ , whose cross-sectional view is given in Fig. 2(e). All of these shells are semiconducting. It is worth noting that the intertubular distances are not of the same value. They vary from 0.42 nm to 0.5 nm and to 0.36 nm from the outermost shell to the innermost shell of the nanotube.

The procedure presented here for determining the atomic structure of the quadruple-walled carbon nanotube can be extended to multiwalled carbon nanotubes with fewer or more shells. With the precision given in the present measurement, up to 15 shells (outer diameter up to 10 nm) can be determined unambiguously. Once the atomic structure of a multiwalled carbon nanotube is determined, we can predict their physical and chemical properties, including identifying which shell is metallic or semiconducting.

Rapid and accurate determination of the atomic structure of multiwalled carbon nanotubes presented here will also be useful for understanding the mechanisms of formation and growth of multiwalled carbon nanotubes.<sup>21,22</sup>

<sup>1</sup>S. Iijima, *Nature (London)* **354**, 56 (1991).

<sup>2</sup>R. Saito, G. Dresselhaus, and M. S. Dresselhaus, *Physical Properties of Carbon Nanotubes* (Imperial College Press, London, 1998).

<sup>3</sup>R. H. Baughman, A. A. Zakhidov, and W. A. de Heer, *Science* **297**, 787 (2002).

<sup>4</sup>R. Saito, M. Fujita, G. Dresselhaus, and M. S. Dresselhaus, *Appl. Phys. Lett.* **60**, 2204 (1992).

<sup>5</sup>L.-C. Qin, X. Zhao, K. Hirahara, Y. Miyamoto, Y. Ando, and S. Iijima, *Nature (London)* **408**, 50 (2000).

<sup>6</sup>N. Hamada, A. Sawada, and A. Oshiyama, *Phys. Rev. Lett.* **68**, 1579 (1992).

<sup>7</sup>R. Saito, M. Fujita, G. Dresselhaus, and M. S. Dresselhaus, *Appl. Phys. Lett.* **60**, 2204 (1992).

<sup>8</sup>L.-C. Qin, S. Iijima, H. Kataura, Y. Maniwa, S. Suzuki, and Y. Achiba, *Chem. Phys. Lett.* **268**, 101 (1997).

<sup>9</sup>J. M. Cowley, P. Nikolaev, A. Thess, and R. E. Smalley, *Chem. Phys. Lett.* **265**, 379 (1997).

<sup>10</sup>J.-F. Colomer, L. Henrard, P. Lambin, and G. Van Tendeloo, *Phys. Rev. B* **64**, 125425 (2001).

<sup>11</sup>M. Gao, J. M. Zuo, R. D. Twisten, I. Petrov, L. A. Nagahara, and R. Zhang, *Appl. Phys. Lett.* **82**, 2703 (2003).

<sup>12</sup>D. Bernaerts, M. O. de Beeck, S. Amelinckx, J. Van Landuyt, and G. Van Tendeloo, *Philos. Mag. A* **74**, 723 (1996).

<sup>13</sup>M. Kociak, K. Suenaga, K. Hirahara, Y. Saito, T. Nakahira, and S. Iijima, *Phys. Rev. Lett.* **89**, 155501 (2002).

<sup>14</sup>J. M. Zuo, I. Vartanyants, M. Gao, R. Zhang, and L. A. Nagahara, *Science* **300**, 1419 (2003).

<sup>15</sup>D. Ugarte, *Nature (London)* **359**, 707 (1992).

<sup>16</sup>B. W. Smith and D. E. Luzzi, *J. Appl. Phys.* **90**, 3509 (2001).

<sup>17</sup>F. Banhart, *Rep. Prog. Phys.* **62**, 1181 (1999).

<sup>18</sup>L.-C. Qin, *J. Mater. Res.* **9**, 2450 (1994).

<sup>19</sup>A. A. Lucas, V. Bruyninckx, and P. Lambin, *Europhys. Lett.* **35**, 355 (1996).

<sup>20</sup>L.-C. Qin, *Chem. Phys. Lett.* **297**, 23 (1998).

<sup>21</sup>S. Iijima, P. M. Ajayan, and T. Ichihashi, *Phys. Rev. Lett.* **69**, 3100 (1992).

<sup>22</sup>T. Guo, P. Nikolaev, A. G. Rinzler, D. Tomanek, D. T. Colbert, and R. E. Smalley, *J. Phys. Chem.* **99**, 10694 (1995).